AD-A123 512 CURE MONITORING AND CONTROL WITH COMBINED 1/1
DIELECTRIC/TEMPERATURE PROBES(U) MASSACHUSETTS INST OF
TECH CAMBRIDGE CENTER FOR MATERIALS SCI..
UNCLASSIFIED S D SENTURIA ET AL. 10 JAN 83 TR-6 F/G 11/4 NL

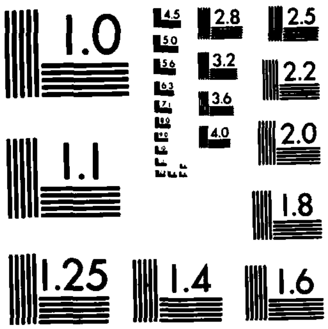

MICROCOPY RESOLUTION TEST CHART
NATIONAL BUREAU OF STANDARDS-1963-A

12

OFFICE OF NAVAL RESEARCH

Contract N00014-78-C-0591

Task No. NR 356-691

TECHNICAL REPORT NO. 6

CURE MONITORING AND CONTROL WITH COMBINED DIELECTRIC/TEMPERATURE PROBES

By

Stephen D. Senturia, Norman F. Sheppard, Jr.,
Huan L. Lee, and Steven B. Marshall

Article prepared for presentation at

The 1983 SAMPE Meeting, Anaheim, CA, April 1983

MASSACHUSETTS INSTITUTE OF TECHNOLOGY
Department of Electrical Engineering and Computer Science
and Center for Materials Science and Engineering
Cambridge, Massachusetts

January 10, 1983

UNCLASSIFIED

SECURITY CLASSIFICATION OF THIS PAGE (*When Data Entered*)

REPORT DOCUMENTATION PAGE

READ INSTRUCTIONS BEFORE COMPLETING FORM

1. REPORT NUMBER

2. GOVT ACCESSION NO. AD-A123522

3. RECIPIENT'S CATALOG NUMBER

4. TITLE (*and Subtitle*)
Cure Monitoring and Control with
Combined Dielectric/Temperature Probes

5. TYPE OF REPORT & PERIOD COVERED
Technical Report
6/82 - 12/82

6. PERFORMING ORG. REPORT NUMBER
Technical Report No. 6

7. AUTHOR(s)
Stephen D. Senturia, Norman F. Sheppard, Jr.,
Huan L. Lee, and Steven B. Marshall

8. CONTRACT OR GRANT NUMBER(s)
N00014-78-C-0591

9. PERFORMING ORGANIZATION NAME AND ADDRESS
Massachusetts Institute of Technology
Department of Electrical Engineering and Computer
Science, Cambridge MA 02139

10. PROGRAM ELEMENT, PROJECT, TASK AREA & WORK UNIT NUMBERS
NR 356-691

11. CONTROLLING OFFICE NAME AND ADDRESS
Department of the Navy, Office of Naval Research
800 N. Quincy Street, Arlington VA 22217
Code 427

12. REPORT DATE
January 10, 1983

13. NUMBER OF PAGES
11

14. MONITORING AGENCY NAME & ADDRESS(*if different from Controlling Office*)

15. SECURITY CLASS. (*of this report*)
UNCLASSIFIED

15a. DECLASSIFICATION/DOWNGRADING SCHEDULE

16. DISTRIBUTION STATEMENT (*of this Report*)
This document has been approved for public release and sale; its distrubtion is unlimited

17. DISTRIBUTION STATEMENT (*of the abstract entered in Block 20, if different from Report*)

18. SUPPLEMENTARY NOTES

19. KEY WORDS (*Continue on reverse side if necessary and identify by block number*)
Dielectrometry, cure monitoring, microdielectrometry, conductivity, permittivit
loss factor, resins, temperature measurement

20. ABSTRACT (*Continue on reverse side if necessary and identify by block number*)

The dielectric and conductive properties of resins used as adhesives and as matrices in composites undergo large changes during cure. The use of these changing electrical properties to monitor cure is a well established technique. The most common structure for such measurements is a parallel plate capacitor using fixed metal plates or metal foils. A relatively new alternative structure is the "Microdielectrometer chip", a miniature integrated circuit probe that can be embedded in the sample under test. (over)

Block 20, Abstract (continued)

This paper reports a new development in Microdielectrometry technology, the addition of a temperature sensor to the probe. The combined dielectric/temperature probe provides highly localized measurements of both temperature and changing dielectric properties. Data are presented that illustrate the use of the Microdielectrometer to detect the viscosity minimum during cure of staged prepreg resin, and the use of the on-chip temperature feature to provide feedback control signals during a test cure.

CURE MONITORING AND CONTROL
WITH COMBINED DIELECTRIC/TEMPERATURE PROBES

Stephen D. Senturia, Norman F. Sheppard, Jr.,
Huan L. Lee, and Steven B. Marshall
Department of Electrical Engineering and Computer Science
and
Center for Materials Science and Engineering
Massachusetts Institute of Technology
Cambridge, MA 02139

ABSTRACT

The dielectric and conductive properties of resins used as adhesives and as matrices in composites undergo large changes during cure. The use of these changing electrical properties to monitor cure is a well established technique. The most common structure for such measurements is a parallel plate capacitor using fixed metal plates or metal foils. A relatively new alternative structure is the "Microdielectrometer chip", a miniature integrated circuit probe that can be embedded in the sample under test. This paper reports a new development in Microdielectrometry technology, the addition of a temperature sensor to the probe. The combined dielectric/temperature probe provides highly localized measurements of both temperature and changing dielectric properties. Data are presented that illustrate the use of the Microdielectrometer to detect the viscosity minimum during cure of staged prepreg resin, and the use of the on-chip temperature feature to provide feedback control signals during a test cure.

Keywords: Cure monitoring and control, dielectric sensor, temperature sensor.

1. INTRODUCTION

The large changes that occur in the dielectric and conductive properties of resins and structural adhesives during cure are well known. Several methods of monitoring cure based on these changing electrical properties have been reported. Ion graphing is a technique which monitors the dramatic drop in DC conductivity that occurs when a resin gels (1). This same conductivity change can be observed in conventional AC dielectric measurements at sufficiently low frequencies, using either parallel-plate capacitor geometries (2,3,4), or using integrated circuit Microdielectrometer probes (5,6). In addition to the conductivity changes, there are clearly observable changes in dielectric permittivity due to the increased hindrance to dipole rotation as resins vitrify. Associated with this effect is a peak in the dielectric loss factor.

Temperature plays a key role in dielectric cure monitoring, and not simply because of the obvious temperature dependence of all reaction rates. The low-frequency conductivity of resins and the relaxation times associated with dipole rotation are intrinsically temperature dependent as well as dependent on the state of cure. Therefore, proper interpretation of dielectric cure data requires knowledge of the temperature. In large parts, temperature gradients set up by the exothermic cure reaction can modify reaction rates and can also modify dielectric properties. It would be desirable, therefore, to be able to make temperature measurements at the same point in the resin from which dielectric signals are being obtained. This paper reports a new Microdielectrometer chip which incorporates an elementary temperature sensor, thereby permitting highly localized combined dielectric/temperature measurements from a single probe.

2. BACKGROUND

2.1 Measurement of Dielectric Properties

In a parallel-plate geometry, the pair of plates form a circuit element which can be represented as a capacitor in parallel with a conductor. The capacitance of the capacitor depends on the area of the plates, the spacing between the plates, and on the dielectric permittivity ε' of the medium between the plates. The conductance of the conductor in parallel with the capacitor depends similarly on the plate area and spacing, and also depends on the conductivity of the medium σ. A conventional way of relating the permittivity and conductivity contributions to one another is to define a quantity with the same dimensions as ε', but proportional to conductivity. From basic electromagnetic theory, the correct corresponding quantity, called the loss factor and denoted by ε'', is equal to σ/ω, where ω is the angular frequency at which both ε' and ε'' are measured. Both ε' and ε'' are usually reported in units of the permittivity of free space, ε_o, which has the value 8.85×10^{-14} Farads/cm. In this case, the ε' value corresponds to the conventionally defined dielectric constant, and a material with an ε'' value of unity at a frequency of 1 Hz has a conductivity equal to 5.56×10^{-13} (Ohm cm)$^{-1}$.

Because both the capacitance and conductance measured from parallel plates depend directly on plate spacing, and becase this spacing typically changes during a cure cycle either by shrinkage of the curing material or through the application of pressure, one usually finds reports of the ratio of ε'' to ε', called the loss tangent (or, conventionally, $\tan\delta$). An equivalent quantity is the dissipation factor of the capacitor, often denoted by D. The benefit in working with $\tan\delta$ is that it is independent of plate spacing, at least to first order. The disadvantage of working with $\tan\delta$ is that when one observes a change, one does not know whether to attribute that change to ε' or to ε'', or to both. Because the conductivity contributes directly to ε'', and can also introduce artifacts in ε' early in cure (see below), it is highly desirable to separate ε' from ε''. The accuracy of this separation with parallel plates depends on knowing and stabilizing the plate area and spacing.

The Microdielectrometry approach to dielectric measurements was first reported at the 1981 SAMPE meeting (5). A miniature integrated circuit (2x4 mm in the new design) contains a pair of interdigitated electrodes, one of which is driven with the AC signal, the other of which serves to collect charge. On-chip amplifiers and off-chip electronic circuitry permit the equivalent of 0.1 pF capacitors to be measured at frequencies as low as 1 Hz with good signal to noise ratio. Because the electrodes are rigid, and are manufactured with microelectronic precision, the intrinsic calibration of the sensor is stable with respect both to temperature and pressure variations. Thus, with the Microdielectrometer, direct separation of ε' from ε'' is always possible. There is no need to combine the measured quantities into $\tan\delta$ to cancel out electrode spacing variations.

Both parallel plate and microdielectrometer structures measure the same basic quantities, ε' and ε'', which can be expessed as

$$\varepsilon' = \varepsilon_\infty + \varepsilon'_{\text{dipole}} \qquad (2.1)$$

$$\varepsilon'' = \frac{\sigma}{\omega} + \varepsilon''_{\text{dipole}} \qquad (2.2)$$

where ε_∞ is the high frequency dielectric permittivity, σ is the conductivity and ω is the angular frequency. The last term in each expression is the contribution of dipole orientation to the dielectric properties. For dipoles having a single relaxation time τ, Debye (7) proposed that these should be

$$\varepsilon'_{\text{dipole}} = \frac{(\varepsilon_0 - \varepsilon_\infty)}{1 + (\omega\tau)^2} \qquad (2.3)$$

$$\varepsilon''_{\text{dipole}} = \frac{(\varepsilon_0 - \varepsilon_\infty)\omega\tau}{1 + (\omega\tau)^2} \qquad (2.4)$$

where ε_0 is the low frequency dielectric permittivity. Note that for $\omega\tau=1$, ε'_{dipole} is half of $(\varepsilon_0 - \varepsilon_\infty)$ and ε''_{dipole} attains its maximum value. In the calculations below a modified form of the Debye equations, proposed by Cole and Cole (8), are used. The modified expressions include an additional parameter, β, which accounts for the distribution of relaxation times in real materials.

In order to provide some insight into what these equations mean, Figure 1 shows a plot of the variation of ε' and of $\log\varepsilon''$ versus isothermal cure time at four frequencies for an idealized material in which the conductivity is assumed to decay exponentially with time (due to cross linking), and the dipole relaxation time is assumed to increase exponentially with time. Numerical values typical of the cure of DGEBA with menthane diamine at 90°C were used to make the plots (the actual data are discussed in the following paragraph). Note the classical dipole relaxation in ε', occuring later in time at successively lower frequencies because of the increase in τ with cure time. Note also that early in cure, the ε'' at each frequency decays exponenti-

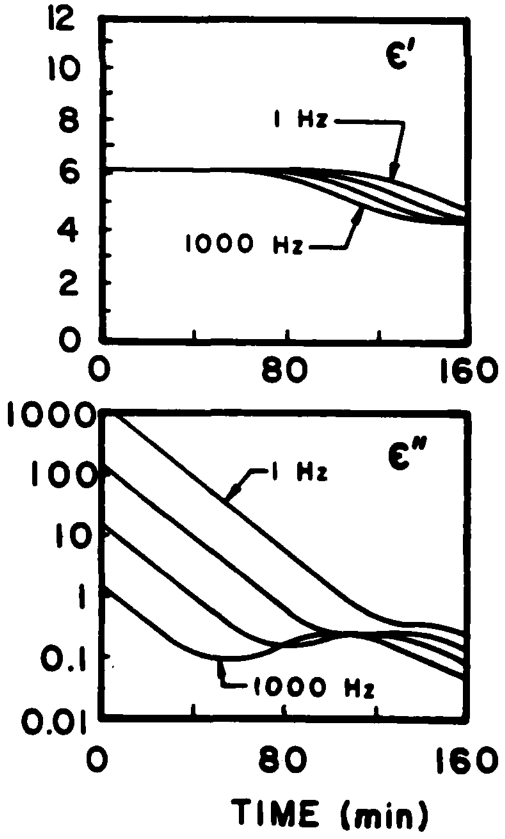

Fig. 1 ε' and ε'' versus time for the model of Eqs. 2.1 and 2.2, with parameters to match Fig. 2 data. Frequencies are 1,10,100 and 1000 Hz

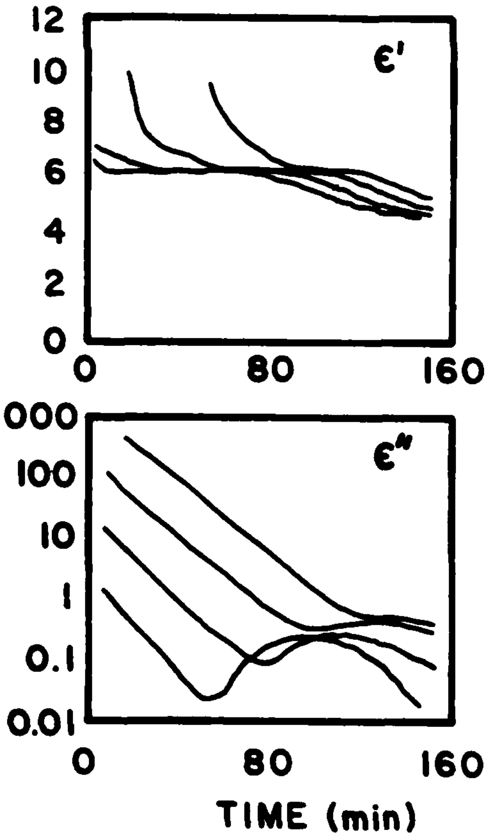

Fig. 2 ε' and ε'' versus time for DGEBA cured with menthane diamine at 90°C.

ally with time (following the conductivity contribution), and that the ε'' value at any time appears to be equal to a constant divided by frequency (that is, an increase in frequency by a factor of 10 produces a corresponding drop in ε'' by a factor of 10). This frequency dependence assures that the effect being observed is a conductivity rather than a dipole loss. Note, however, that later in cure, loss peaks due to the dipole orientation are observed, particularly at higher frequencies.

Experimental behavior is very similar to this ideal model. Figure 2 shows plots corresponding to the model curves of Fig. 1 for DGEBA cured with menthane diamine at 90°C. The overall resemblance is immediately noticable. Two differences are evident, however. Early in cure, the experimental ε' value is much larger than ε_0, which has a value of 6.5 in this example. The reason for this is believed to be that the electrodes are blocking, and that the ions that give rise to the bulk conductivity accumulate at the electrodes. This effect is well known in electrolytes (9). From an experimental point of view, we usually observe very large ε' in the presence of large ε''. A second difference between the model and experiment is that late in cure, the changes in properties appear to slow down and cease. This is consistent with a decrease in reaction rate after vitrification, which was not included in the simple illustrative model.

From the above example, it is clear that by observing ε'' at several different frequencies, one can identify whether one is observing a conductivity or a dipole loss. An important additional fact is that this conductivity is well correlated with the viscosity of the medium (6,10). Thus, when curing a prepreg, one should expect a peak in ε'' corresponding to the viscosity minimum. An example of such a result is presented in Section 3.1 below.

2.2 Temperature Measurement with Diodes

Semiconductor diodes have current-voltage characteristics with a sufficiently stable and predictable temperature dependence to permit their use as thermometers. If the the diode carries a forward current that is large enough to mask surface and space-charge recombination effects, and at the same time small enough to avoid high-level injection phenomena, then at a fixed current the variation of forward biased voltage with temperature is derivable from basic theory, and equals -2.3 mV/°C. Ideally, one need only calibrate the forward voltage at one temperature, such as room temperature, but in practice, parasitic effects may lead to small departures from the theoretical temperature dependence.

Because the Microdielectrometer probe is an integrated circuit, a temperature sensor diode can be incorporated in the probe itself, using the same fabrication procedure. The photomicrograph of Figure 3 shows the top view of the present sensor. Of particular interest are the interdigitated electrodes used to measure dielectric properties, and the added diode used to measure temperature. The substrate on which these devices are fabricated is silicon, and is a good thermal conductor. Therefore, the diode and electrode temperatures cannot be significantly different. The center-to-center distance between the diode and the elelectrode array is only 0.04 mm.

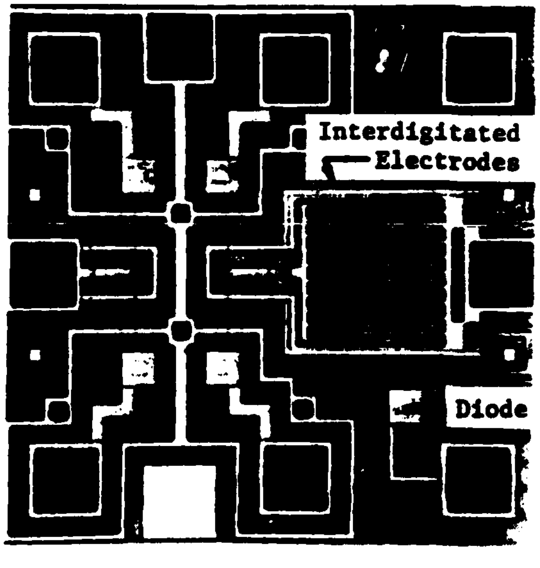

Fig. 3 Microdielectrometer

Figure 4 shows a calibration curve for two different diodes, one uncoated and one coated with cured DGEBA/MPDA resin. The voltage variation is plotted relative to the forward voltage at 20°C. The forward current is fixed at 100 microamps. A least-squares best fit line was calculated from the data for each diode, and in both cases the slope was -2.26 mV/°C, indicating ideal behavior. Our usual procedure is to measure the forward voltage at room temperature prior to a cure experiment, and then to use the 2.26 mV/°C slope to determine the temperature from the diode forward voltage. Over the range 20°C to 180°C, this yields results that should be accurate to better than 2°C. The incremental sensitivity of the temperature sensor is 0.2°C. For absolute accuracy in the 0.2°C range, a more complete calibration would be required.

3. EXPERIMENTAL RESULTS

3.1 Cure of Staged Prepreg Resin

As an illustration of the use of the combined dielectric/temperature probe in the present version of the Microdielectrometer chip, a ramped cure of a staged prepreg resin was carried out. Samples of epoxy-glass prepreg were obtained from a circuit-board laminate manufacturer. The basic formulation is a brominated epoxy resin cured with DICY. The prepreg cloth had been coated and staged. Several sheets of the cloth were

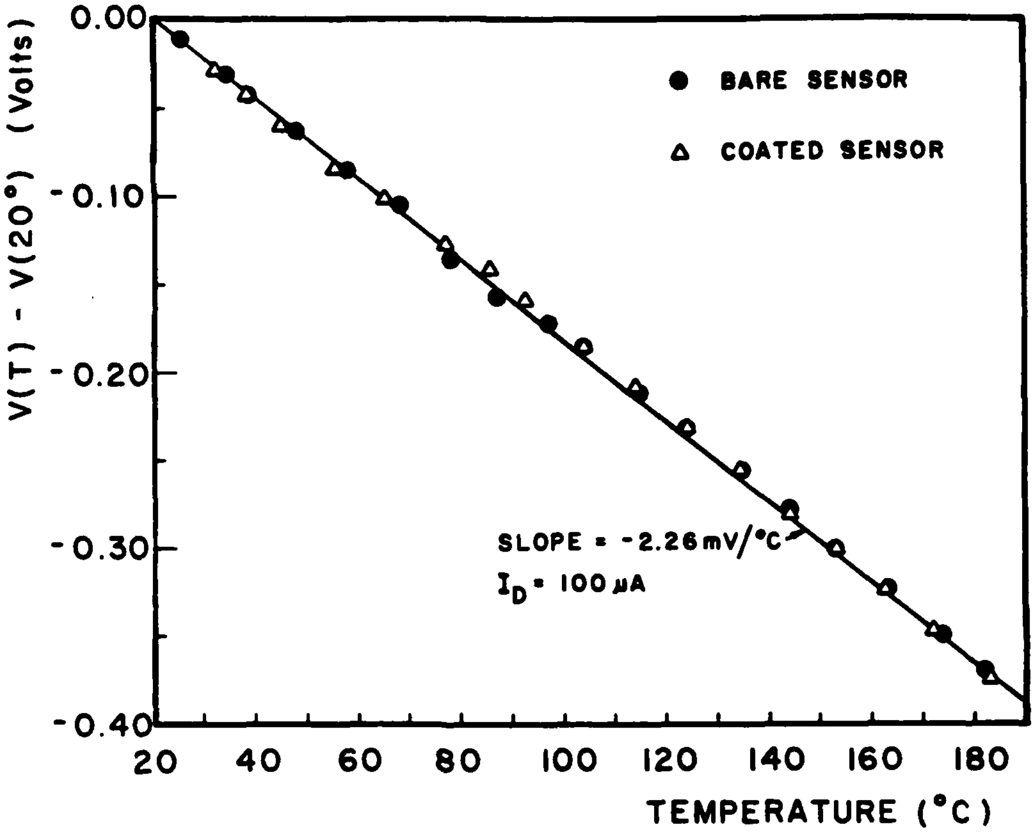

Fig. 4 Diode forward voltage versus temperature at fixed current of 100 μA for both uncoated and resin-coated devices.

crumbled to collect the resin, which at this point was in the form of a coarse powder. Some of the powder was placed directly on the surface of a Microdielectrometer chip. The probe was placed in an oven and the temperature was ramped at a rate of 2°C per minute from 70°C to 170°C, then held. Signals were obtained as soon as the resin began to melt and flow onto the chip surface. Figure 5 shows a plot of temperature and loss factor versus time. The frequency dependence of the loss factor corresponds to conductivity rather than dipole orientation. Early in cure, this conductivity increases steadily as the viscosity decreases due to the temperature rise. As the cure proceeds, the conductivity reaches a maximum, then begins to decrease. This indicates that the increase in viscosity due to crosslinking is beginning to dominate the intrinsic temperature dependence of the viscosity. The results demonstrate the suitability of the microdielectrometer for obtaining process control data during cure.

3.2 Cure Control Experiments

The on-chip temperature sensor provides an interesting capability

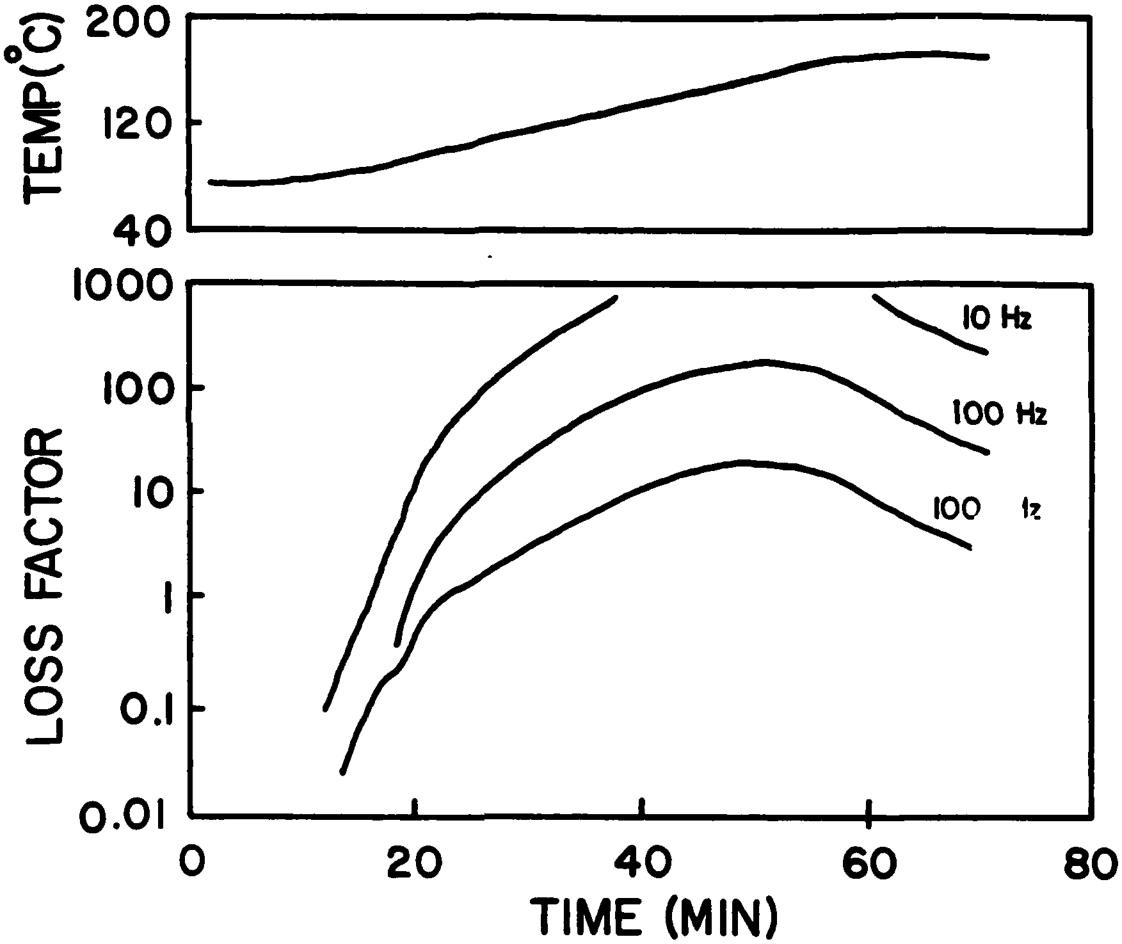

Fig. 5 Loss factor and temprature versus time for ramped prepreg cure.

for closed-loop control. As a test of this capability, the following experiment was performed (11). A pair of Microdielectrometer chips was bonded within a single 16-pin ceramic DIP package. A photomicrograph is shown in Figure 6. One of the chips was used as a heater/controller, with 3 Watts of 20 kHz AC power dissipation in the on-chip transistors being used to heat the chip, the ceramic substrate, and the other chip bonded to the substrate. A switching controller used the temperature signal derived from the diode in the heater/controller chip to

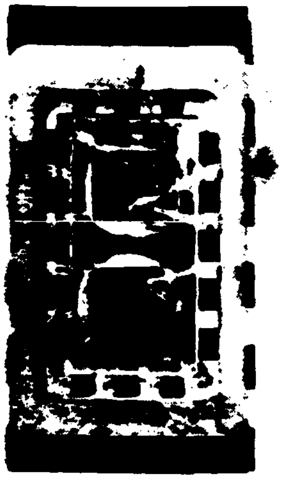

Fig. 6 "Microclave" showing dielectric sensor, top, and heater/controller, bottom.

achieve regulation of better than 1°C. The second microdielectrometer chip was used as a cure monitor, with its on-chip temperature sensor making an independent measurement of the actual temperature at the cure-monitoring electrodes. Thus the entire cure-monitoring test station, including the function of the oven, was merged into a single integrated circuit package, which we have called the "Microclave". The resin used for this experiment was DGEBA cured with MPDA. Figures 7 and 8 show the dielectric permittivity and loss factor data obtained from this experiment. Note that all of the features seen in Figure 2 are also observed in this experiment. Such an assembly would make a particularly compact test station for quality assurance inspection of resins.

4. CONCLUSIONS

In viewing the results presented above, it is important to keep several issues in mind. First, the frequency dependence of ε'' is a particularly useful experimental quantity to monitor. From it, one can be certain whether one is observing conductivity or dipole orientation effects. Second, early in cure, conductivity as revealed in the loss factor correlates with viscosity, and can potentially be used for cure control (for example, to locate the viscosity minimum in prepreg). Third, parallel plate techniques of measurement are better suited for loss tangent measurement than for loss factor measurement, because the plate spacing may not be either accurately known, or may not be constant in typical cure cycles. When the permittivity is itself changing with cure, as happens with conductivity-induced artifacts as in Figure 2, then the behavior of the loss tangent is complex, and less easily interpretable. Fourth, the fixed electrode geometry of the Microdielectrometer provides for direct observation of loss factor, with the effects of temperature and pressure variation cancelled by differential measurement techniques. Finally, the Microdielectrometer technology provides for easy incorporation of moderate accuracy semiconductor diode temperature sensors into a combined dielectric/temperature probe. The probe is implantable, makes a highly localized measurement of both dielectric properties and temperature, and provides both kinds of signals for potential cure-control applications.

5. ACKNOWLEDGEMENTS

This work was supported in part by the Office of Naval Research. Devices were fabricated both at MIT in the Microelectronics Laboratory of the Center for Materials Science and Engineering, which is supported in part by the National Science Foundation under

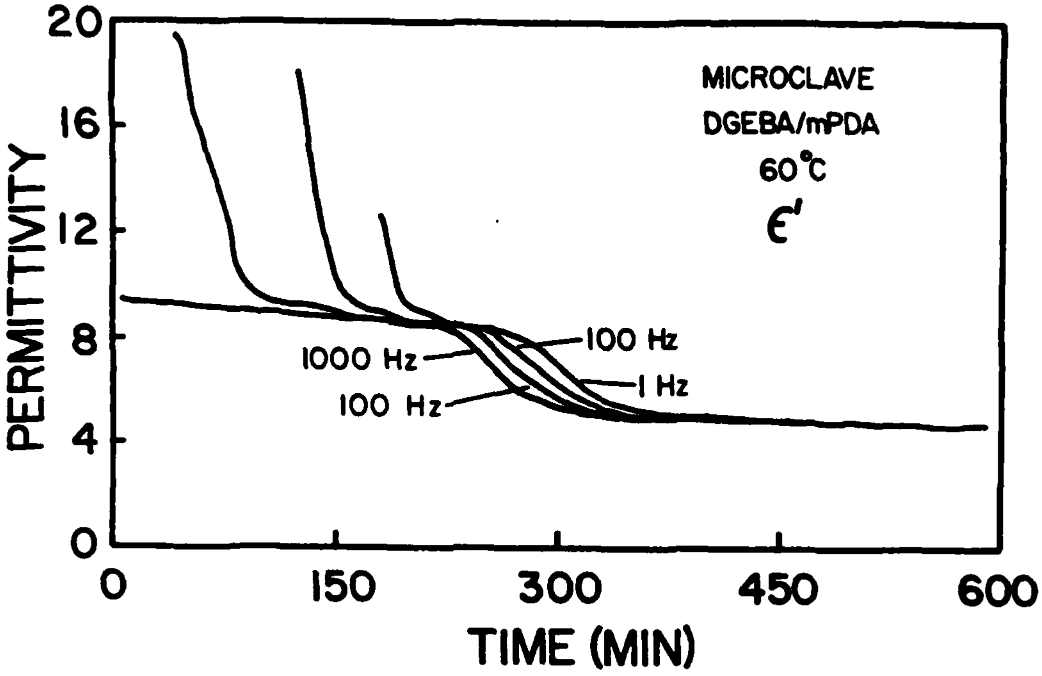

Fig. 7 ε' versus time for DGEBA/MPDA cured in "Microclave"

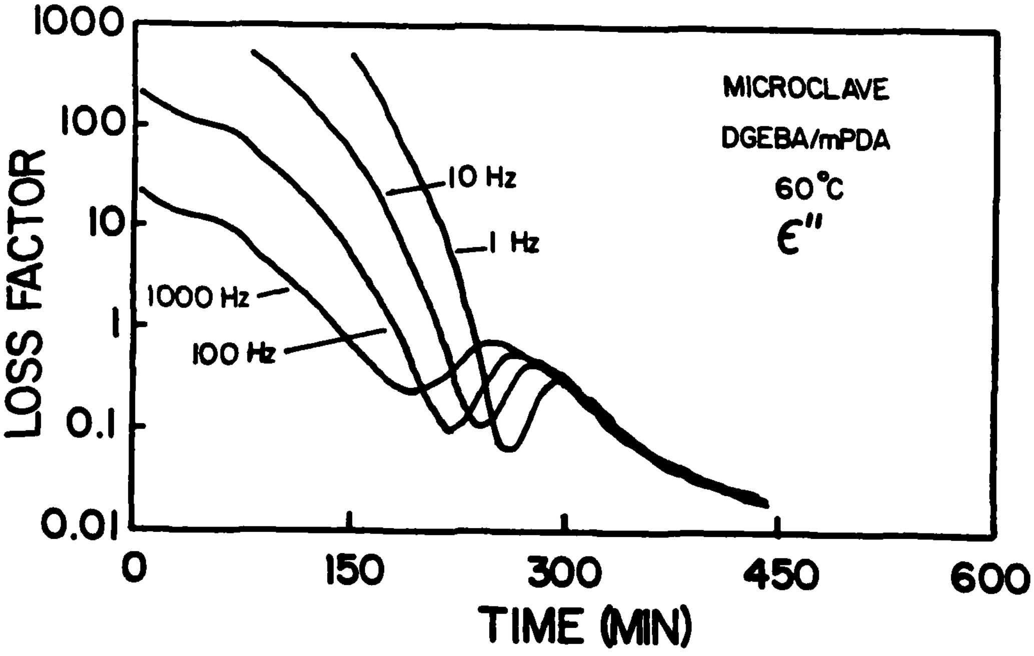

Fig. 8 ε" versus time for DGEBA/MPDA cured in "Microclave"

Contract DMR 81-19295, and at Texas Instruments, Dallas, TX. We are indebted to Mr. L. Hutter of TI for his assistance. Some of the Microdielectrometry equipment was purchased under NSF Contract ENG-7717219. Samples of the DGEBA-menthane diamine were obtained from D. Roylance and T. Donnelan of MIT; the DGEBA-MPDA resins were obtained from Dr. N. Schneider at AMMRC, Watertown, MA.

6. REFERENCES

1. M. Acitelli, R. B. Prime and E. Sacher, Polymer, 12, 335 (1971).

2. C. A. May, Proc. 21st SAMPE Symposium, p. 803, *Los Angeles*, 1976.

3. L. D. Dragatakis and Z. N. Sanjana, Insulation/Circuits, p. 27, Jan 1978.

4. S. A. Yalof, Chemtech, p. 165, March 1975.

5. N. F. Sheppard, S. L. Garverick, D. R. Day and S. D. Senturia, Proc. 26th SAMPE Symposium, p. 65, Los Angeles, 1981.

6. N. F. Sheppard, D. R. Day, H. L. Lee and S. D. Senturia, Sensors and Actuators, 2, 263 (1982).

7. P. Debye, Polar Molecules, Chemical Catalog Co., New York (1929).

8. K. S. Cole and R. H. Cole, J. Chem. Phys. 9, 341 (1941).

9. J. R. Macdonald, J. Chem. Phys., 54(5), 2026 (1971).

10. R. J. Armstrong, Solid State Technology, November 1969, p. 50.

11. S. B. Marshall, S. B. Thesis, MIT, (1982), unpublished.

7. BIOGRAPHIES

Stephen D. Senturia is a Professor of Electrical Engineering at MIT, having received an S.B. in Physics from Harvard (1961), and a Ph.D. in Physics from MIT (1966).

Norman F. Sheppard, Jr. is presently a graduate student in the MIT Department of Electrical Engineering and Computer Science, having received an S.B. (1978) and an S.M. (1979) in Chemical Engineering from MIT, and an S.M. (1981) and an E.E. (1981) in Electrical Engineering from MIT.

Huan L. Lee received an S.B. (1979) from UCLA, and an S.M. (1982) and an E.E. (1982) from MIT Department of Electrical Engineering and Computer Science. He is currently an employee of Micromet Instruments, Inc.

Steven B. Marshall received an S.B. (1982) from the MIT Department of Electrical Engineering and Computer Science.

TECHNICAL REPORT DISTRIBUTION LIST, GEN

No. Copies

Office of Naval Research (2)
Attn: Code 413
800 North Quincy Street
Arlington, VA 22217

ONR Pasadena Detachment (1)
Attn: Dr. R. J. Marcus
1030 East Green Street
Pasadena, CA 91106

Commander, Naval Air Systems Command (1)
Attn: Code 310C (H. Rosenwasser)
Department of the Navy
Washington, DC 20360

Defense Technical Information Center (12)
Building 5, Cameron Station
Alexandria, VA 22314

Dr. Fred Saalfeld (1)
Chemistry Division, Code 6100
Naval Research Laboratory
Washington, DC 20375

U.S. Army Research Office (1)
Attn: CRD-AA-IP
P. O. Box 12211
Research Triangle Park, NC 27709

Mr. Vincent Schaper (1)
DTNSRDC Code 2803
Annapolis, MD 21402
Chicago, IL 60605

Naval Ocean Systems Center (1)
Attn: Dr. S. Yamamoto,
Marine Sciences Division
San Diego, CA 91232

No. Copies

Naval Ocean Systems Center (1)
Attn: Mr. Joe McCartney
San Diego, CA 92152

Naval Weapons Center (1)
Attn: Dr. A. B. Amster,
Chemistry Division
China Lake, CA 93555

Naval Civil Engineering Laboratory (1)
Attn: Dr. R. W. Drisko
Port Hueneme, CA 93401

Dean William Tolles (1)
Naval Postgraduate School
Monterey, CA 93940

Mr. John Boyle (1)
Materials Branch
Naval Ship Engineering Center
Philadelphia, PA 19112

Scientific Advisor (1)
Commandant of the Marine Corps
(Code RD-1)
Washington, DC 20380

Naval Ship Research and Development (1)
Center
Attn: Dr. G. Bosmajian, Applied
Chemistry Division
Annapolis, MD 21401

Mr. A. M. Anzalone (1)
Administrative Librarian
PLASTEC/ARRADCOM
Bldg 3401
Dover, NJ 07801

TECHNICAL REPORT DISTRIBUTION LIST, GEN

No. Copies

Dr. E. Baer (1)
Department of Macromolecular Science
Case Western Reserve University
Cleveland, OH 44106

Dr. M. Broadhurst (2)
Bulk Properties Section
National Bureau of Standards
U.S. Department of Commerce
Washington, DC 20234

Dr. K. D. Pae (1)
Department of Mechanics and
Materials Science
Rutgers University
New Brunswick, NJ 08903

Naval Surface Weapons Center (1)
Attn: Dr. J. M. Augl, Dr. B. Hartman
White Oak
Silver Spring, MD 20910

Dr. G. Goodman (1)
Globe Union Incorporated
5757 North Green Bay Avenue
Milwaukee, Wisconsin 53201

Prof. Hatsuo Ishida (1)
Department of Macromolecular Science
Case-Western Reserve University
Cleveland, OH 44106

Dr. John Lundberg (1)
School of Textile Engineering
Georgia Institute of Technology
Atlanta, GA 30332

Dr. C. Giori (1)
IIT Research Institute
10 West 35 Street
Chicago, IL 60616

Dr. R. S. Roe (1)
Department of Materials Science
and Metallurgical Engineering
University of Cincinnati
Cincinnati, OH 45221

No. Copies

Picatinny Arsenal (1)
Attn: A. M. Anzalone, Bldg. 3401
SMUPA-FR-M-D
Dover, NJ 07801

Dr. J. K. Gillham (1)
Department of Chemistry
Princeton University
Princeton, NJ 08540

NASA-Lewis Research Center (1)
Attn: Dr. T. T. Serofini, MS-49-1
2100 Brookpark Road
Cleveland, OH 44135

Dr. Charles H. Sherman (1)
Code TD 121
Naval Underwater Systems Center
New London, CT 06320

Dr. William Risen (1)
Department of Chemistry
Brown University
Providence, RI 02192

Dr. J. White (1)
Chemical and Metallurgical Engineering
University of Tennessee
Knoxville, TN 37916

Dr. T. J. Reinhart, Jr., Chief (1)
Composite and Fibrous Materials Branch
Nonmetallic Materials Division
Department of the Air Force
Air Force Materials Laboratory (AFSC)
Wright-Patterson AFB, OH 45433

Dr. J. Lando (1)
Department of Macromolecular Science
Case Western Reserve University
Cleveland, OH 44106

Dr. J. A. Manson (1)
Materials Research Center
Lehigh University
Bethlehem, PA 18015

Dr. Robert E. Cohen (1)
Chemical Engineering Department
Massachusetts Institute of Technology
Cambridge, MA 02139

Dr. T. P. Conlon, Jr., Code 3622 (1)
Sandia Laboratories
Sandia Corporation
Albuquerque, NM

Dr. Martin Kaufman (1)
Code 38506
Naval Weapons Center
China Lake, CA 93555

Prof. C. S. Paik Sung (1)
Department of Materials Science and
Engineering, Room 8-109
Massachusetts Institute of Technology
Cambridge, MA 02139

Dr. Curtis W. Frank (1)
Department of Chemical Engineering
Stanford University
Stanford, CA 94035

Mr. Robert W. Jones
Advanced Projects Manager
Hughes Aircraft Company
Mail Station D 132
Culver City, CA 90230

Dr. R. F. Helmreich (1)
Contract RD E
Dow Chemical Co.
Midland, MI 48640

Dr. R. S. Porter (1)
Department of Polymer Science
and Engineering
University of Massachusetts
Amherst, MA 01002

Prof. Garth Wilkes (1)
Department of Chemical Engineering
Virginia Polytechnic Institute and
State University
Blackburg, VA 24061

Dr. David Soong (1)
Department of Chemical Engineering
University of California
Berkeley, CA 94720

Prof. Brian Newman (1)
Department of Mechanics and
Materials Science
Rutgers, The State University
Piscataway, NJ 08854

2-8

DT